



FULL PAPER

Synthesis, characterization, molecular docking and biological activities of novel pyrazoline derivatives

Fikret Turkan¹ | Adnan Cetin² | Parham Taslimi³ | Halide S. Karaman⁴ | İlhami Gulçin⁴¹Health Services Vocational School, Iğdır University, Iğdır, Turkey²Department of Science, Faculty of Education, Muş Alparslan University, Muş, Turkey³Department of Biotechnology, Faculty of Science, Bartın University, Bartın, Turkey⁴Department of Chemistry, Faculty of Science, Atatürk University, Erzurum, Turkey**Correspondences**Fikret Turkan, Health Services Vocational School, Iğdır University, 76000 Iğdır, Turkey.
Email: fikret.turkan@gmail.com**Abstract**

In this study, synthesis of ethyl 2-((4-bromophenyl)diazenyl)-3-oxo-phenylpropanoate **1** was carried out and a series of new 3*H*-pyrazol-3-ones (**P1-7**) were synthesized from **1** as well as various hydrazines. The obtained yields of the synthesized compounds were moderate (40–70%) and these compounds were confirmed by spectral data. These novel pyrazoline derivatives were effective inhibitor compounds of the human carbonic anhydrase I and II isozymes (hCAs I and II) and of the acetylcholinesterase (AChE) enzyme, with K_i values in the range of 17.4–40.7 nM for hCA I, 16.1–55.2 nM for hCA II, and 48.2–84.1 nM for AChE. In silico studies were performed on the compounds inhibiting hCA I, hCA II, and AChE receptors. On the basis of the findings, the inhibition profile of the new pyrazoline compounds at the receptors was determined.

KEYWORDS

acetylcholinesterase, enzyme inhibition, human carbonic anhydrase, in silico study, induced fit docking, pyrazoline

1 | INTRODUCTION

Heterocyclic chemistry has grown very rapidly particularly in the development of synthetic methods and investigation of bioactive properties of the synthesized materials. The compounds having pyrazoline structure are a significant group in the heterocyclic chemistry. These compounds are scaffold target compounds in the field of medicinal and synthetic chemistry.^[1,2] These compounds were used in the development of drug research and agricultural products.^[3-5] In the previous studies, it was indicated that these compounds have significant pharmacological and biological activities.^[6-8] Many pyrazoline compounds are reported to possess a broad spectrum of biological activities such as antimicrobial, antidepressant, neuroprotective, anticonvulsant, anti-inflammatory, analgesic, antitubercular, local anesthetic, hypoglycemic, hypotensive, insecticide, herbicide, and molluscicidal.^[9-16] In addition, the antioxidant properties of the newly synthesized pyrazoline group were also studied.^[17] The pyrazoline derivatives were used as efficient and potent inhibitor of glycogen synthase kinase and they

also were used as a selective inhibitor against to capable of causing bacterial cell death and DNA gyrase.^[18-20] Some known samples including the synthetic pyrazoline dipyrone having feature analgesic are used for preoperative pain.^[21] Propifenazon has been developed for antipyretic anti-inflammatory drugs.^[22] Palerol is used as a novel spasm-analgesic in obstetrics and gynecology.^[23] Nifenazone is utilized for treating rheumatic and analgesic^[24] and muzolimine is used for the treatment of hypertension^[25] and novel N1-substituted 3,5-diphenyl pyrazoline compounds have been synthesized for evaluation as anti-*Helicobacter pylori* agents (Figure 1).^[26]

Carbonic anhydrases (CAs, E.C.4.2.1.1) exist in many living systems and have a diversity of physiological and pathological procedures including fluid balance, neurological disorders, bone resorption, pH regulation, glaucoma, carboxylation reactions, cancer, calcification, osteoporosis, tumorigenicity, and the synthesis of bicarbonate (HCO_3^-).^[27-29] CA isoforms play a significant role in the physiology of coral calcification. CA enzyme has active cofactors in the brain, gastric mucosa, salivary glands, kidney, nerve myelin sheath, eye lens, pancreas, prostate, and uterus.^[30] Also, CA levels

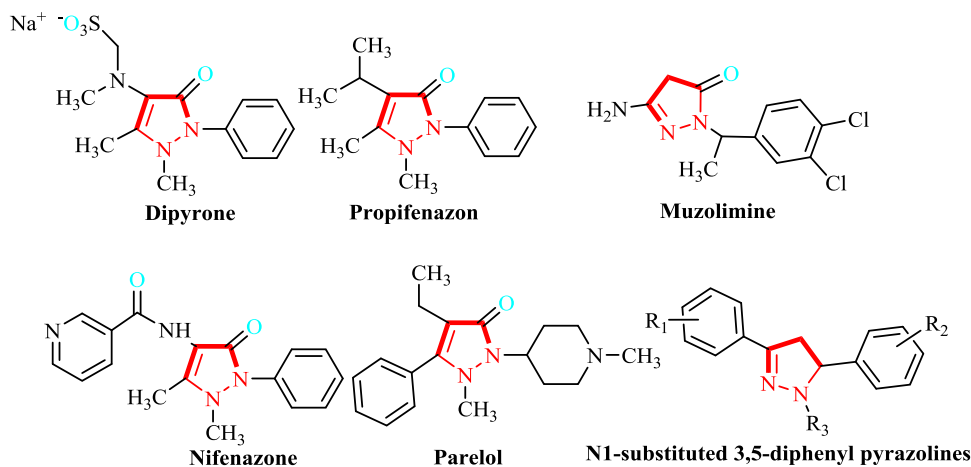


FIGURE 1 The chemical structures of some important pyrazolines



SCHEME 1 Reaction equation of CA

are considerably reduced in the brain tissue cells of patients suffering from Alzheimer's disease (AD), proving an essential involvement of various human carbonic anhydrase isozymes (hCA I, II, IV, and VII) in learning functions and cognition.^[31] CA isoforms are biological catalysts, which convert water (H₂O) and carbon dioxide (CO₂) to a proton (H⁺) and HCO₃⁻ (Scheme 1).^[32-34] This reaction defines to the fastest determined reactions (k_{cat}, 10⁶/s) in the environment and is required to live in plants and animals.^[35]

Cholinesterases (ChE) catalyze the hydrolysis of acetylcholine (ACh) into acetic acid and choline, a fundamental mechanism for the restoration act of the cholinergic neurotransmission.^[36,37] These enzymes include butyrylcholinesterase (E.C.3.1.1.8) and acetylcholinesterase (AChE; E.C.3.1.1.7) enzymes. ACh molecules are synthesized in presynaptic terminals from choline and it is necessary for cholinergic neurotransmission in the peripheral nervous systems and their central. AD is

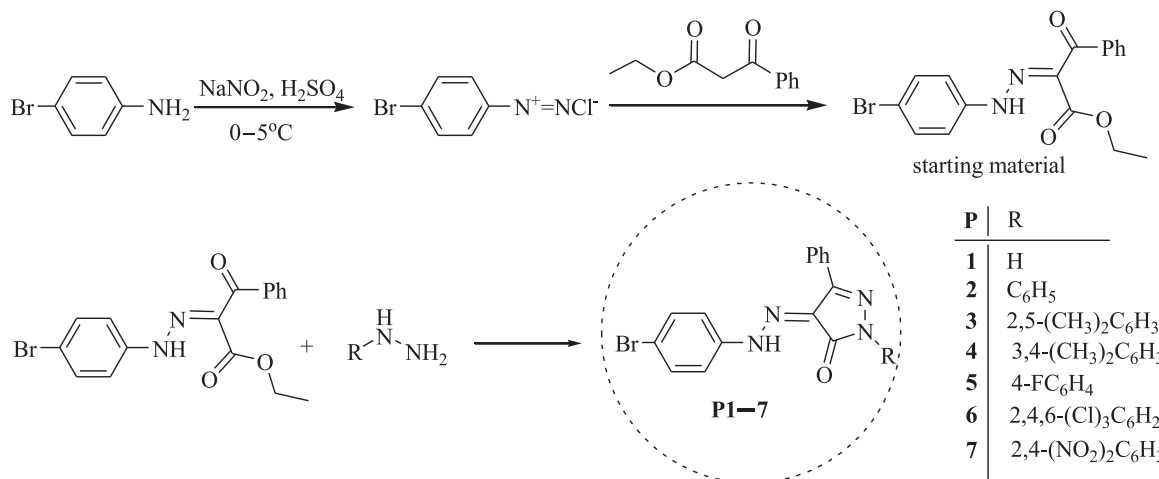
determined by dementia, memory loss and cognitive impairment.^[38,39] Perception is affected in derangements such as AD. A low concentration of ACh can create several neuropsychiatric perturbations and neuropsychological like Parkinson's disease and AD.^[40,41]

In this article, we synthesized some new pyrazoline derivatives (P1-7). In addition, characterized their inhibition confidants against AChE, hCA I, and hCA II, and evaluated their inhibition confidants to acetazolamide (AZA) compound, which is a clinical standard used carbonic anhydrase inhibitor (CAI). On the other hand, tacrine (TAC) molecule was used a control compound for AChE enzyme inhibition.

2 | RESULTS AND DISCUSSION

2.1 | Chemistry

The synthesis of pyrazoline compounds (P1-7) is shown in Scheme 2. Initially starting material ethyl 2-((4-bromophenyl)diazonyl)-3-oxo-phenylpropanoate (**1**) was prepared as result of coupling reaction of ethyl benzoyl acetate and tetra azotized solution which was obtained



SCHEME 2 Synthesis of the pyrazoline derivatives

4-bromoaniline with sodium nitrite solution on the ice bath.^[42] **1** was obtained in good yield 84%.

The IR spectrum of compound **1** showed absorption bands at 3125 cm⁻¹ corresponding to -NH hydrazide, 1721 cm⁻¹ ester and 1670 cm⁻¹ amide carbonyl groups, respectively. The ¹H-NMR spectrum revealed the signal (-NH) protons of hydrazide in the region δ 8.3 ppm, the signals protons of methylene (-CH₂) in the region δ 3.9 ppm, the signals protons of methyl (-CH₃) in the region δ 1.2 ppm, the multiplied signals protons of aromatic ring (-CH) in the region δ 8.0–6.5 ppm. The ¹³C-NMR spectrum revealed the signals carbonyls of benzoyl and ester in the region δ 191.5 and 164.4 ppm, respectively. The signal carbonyl of imine in the region δ 150.7 ppm, the signal of methylene carbon in the region δ 59.7 ppm, the signal of methyl carbon in the region δ 13.4 ppm. Then, the pyrazoline derivatives (**P1–7**) were obtained via cyclocondensation the starting material and various hydrazines (hydrazine hydrate, phenyl hydrazine, 2,5-dimethylphenyl hydrazine, 3,4-dimethyl phenyl hydrazine, 4-trifluoromethyl phenyl hydrazine, 4-bromo phenyl hydrazine, and 2,4-dinitro phenyl hydrazine, respectively) according to the literature.^[6] The yields of pyrazoline derivatives **P1–7** were obtained in 40–70%. The pyrazoline derivatives **P1–7** were characterized by ¹H, ¹³C-NMR, FT-IR, and mass analysis. The IR spectra of synthesized pyrazoline derivatives (**P1–7**) showed corresponding absorption bands 3226–3124 cm⁻¹ -NH imine, 1672–1662 cm⁻¹ pyrazole carbonyl group, and 3082–3060 cm⁻¹ -CH aromatic vibrations, respectively. The ¹H-NMR spectra of **P1–7** revealed the signal protons of -NH in the region δ 8.3–8.00 ppm, the multiplied signals (-CH) protons of aromatic ring in the region δ 8.0–6.5 ppm. The ¹³C-NMR spectrum revealed the signals carbonyls of pyrazole in the region δ 163.4–160.4, the signal carbonyl of imine in the region 150.7 ppm, the signal of methylene carbon in the region δ 59.7 ppm, the signal of methyl carbon in the region 13.4 ppm, the signals (C3) and (C4) of pyrazole ring in the region δ 157.1–155.1 and 153.4–152.6 ppm, respectively. Furthermore, the signals protons of methyl groups for **P3** compound were observed in the region δ 2.3 and 1.5 ppm in ¹H-NMR spectrum and its ¹³C-NMR spectrum revealed the signals of methyl carbons were observed in the region δ 21.5 and 16.6 ppm. Also, for **P5** compound was observed at

δ -62.5 ppm signal by ¹⁹F-NMR spectrum. Finally, synthesized pyrazoline derivatives were confirmed by spectral data in agreement with our previous findings.^[6,43]

2.2 | Biological activity

All the synthesized new pyrazoline derivatives (**P1–7**) were tested to investigate their inhibitory act toward AChE and the slower hCA I and II isoenzymes. The chemical structures of new pyrazoline derivatives (**P1–7**) are seen in Scheme 2 and their AChE, and CA I, and II isoenzymes inhibition data are shown in Table 1. The pyrazoline derivatives (**P1–7**) showed effective inhibition profiles against the enzymes mentioned above. The following results are presented in this part.

Special isoforms from the CA families of zinc metalloenzymes have been dependent on kind of diseases.^[44] Classical CAIs, generally sulfonamide-based compounds and their features were inquired as antiepileptic, antiobesity, antiglaucoma, anticancer compounds, and against antineuropathic pain.^[45] The cytosolic enzyme hCA I was inhibited by the novel pyrazoline derivatives (**P1–7**), with K_i values ranging between 17.42 ± 3.61 and 40.73 ± 8.17 nM. In addition, (Z)-4-(2-(4-bromophenyl)hydrazineylidene)-5-phenyl-2-(2,4,6-trichlorophenyl)-2,4-dihydro-3H-pyrazol-3-one (**P6**) and (Z)-4-(2-(4-bromophenyl)hydrazineylidene)-5-phenyl,4-trifluoromethylphenyl-2,4-dihydro-3H-pyrazol-3-one (**P5**) recorded the most powerful hCA I isoform inhibition properties with K_i values of 17.42 ± 3.61 and 20.14 ± 5.26 nM, respectively (Figure 2). The clinically and standard used drug AZA calculated a K_i value of 75.16 ± 14.44 nM. Thus, the evaluated novel pyrazoline derivatives (**P1–7**) showed better inhibitory profiles when compared to AZA molecule (Table 1 and Figure 3).

The importance of isoenzyme and physiologically dominant cytosolic hCA II enzyme is dependent on different illnesses. The hCA II was impressively inhibited by the novel pyrazoline derivatives (**P1–7**) evaluated here. These molecules were shown to strongly inhibit hCA II, with K_i values ranging from 16.1 ± 2.8 nM to 55.2 ± 12.5 nM. K_i amounts of new molecules are better than those of the standard used drug AZA (K_i: 86.5 ± 21.2 nM). All the evaluated

TABLE 1 HCA I and II and AChE enzyme inhibition values of novel pyrazoline derivatives (**P1–7**)

Com- pounds	IC ₅₀ (nM)		K _i (nM)						
	hCA I	r ²	hCA II	r ²	AChE	r ²	hCA I	hCA II	AChE
P1	24.7	0.9632	32.1	0.9951	108.3	0.9847	30.17 ± 3.8	40.2 ± 10.2	77.1 ± 12.5
P2	30.2	0.9683	40.1	0.9783	122.9	0.9698	36.12 ± 5.0	46.3 ± 8.3	84.1 ± 17.2
P3	33.7	0.9974	45.3	0.9910	104.9	0.9810	40.73 ± 8.2	55.2 ± 12.5	68.3 ± 11.4
P4	27.1	0.9817	35.7	0.9788	97.4	0.9538	28.53 ± 4.9	41.8 ± 7.3	58.1 ± 10.8
P5	17.2	0.9627	23.6	0.9971	82.3	0.9941	20.14 ± 5.3	22.1 ± 3.7	48.2 ± 9.5
P6	12.7	0.9889	16.4	0.9814	85.3	0.9473	17.42 ± 3.6	16.1 ± 2.8	52.7 ± 15.4
P7	29.3	0.9592	33.8	0.9738	100.1	0.9821	32.54 ± 6.9	30.3 ± 5.9	64.4 ± 12.6
AZA ^a	73.5	0.9845	81.5	0.9391	-	-	75.16 ± 14.4	86.5 ± 21.2	-
TAC ^b	-	-	-	-	145.11	0.9721	-	-	89.54 ± 11.1

Note: AChE: acetylcholinesterase; AZA: acetazolamide; hCA I and II: human carbonic anhydrase isoenzymes I and II; TAC: tacrine.

^aAZA was used as a standard inhibitor for hCA I and II.

^bTAC was used as a standard inhibitor for AChE enzyme.

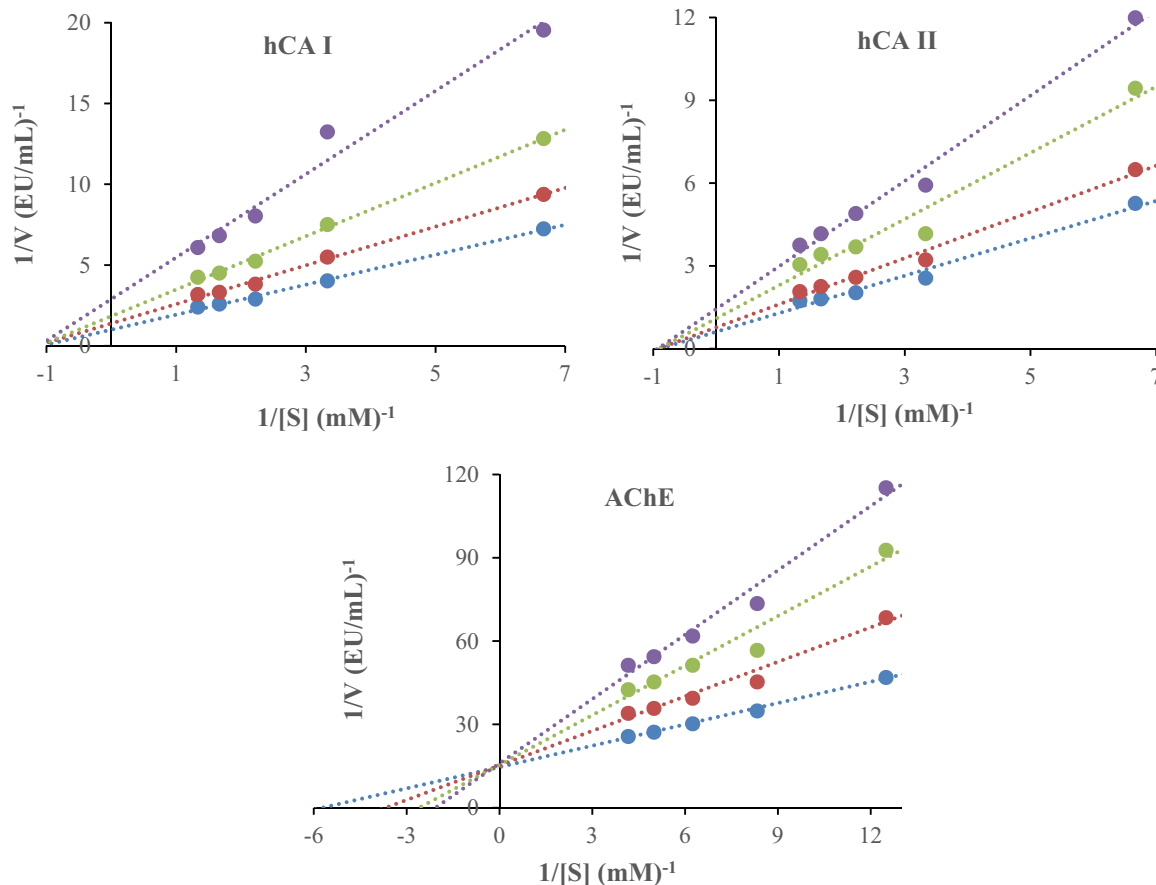


FIGURE 2 Determination of Lineweaver-Burk graphs for novel pyrazoline derivatives (P1–7) against hCA I and II (P6), and AChE (P5) enzyme. AChE: acetylcholinesterase; hCA I and II: human carbonic anhydrase isoenzymes I and II

novel pyrazoline derivatives (P1–7) showed potent inhibition against hCA II, but the compound of (Z)-4-(2-(4-bromophenyl)hydrazineylidene)-5-phenyl-2-(2,4,6-trichlorophenyl)-2,4-dihydro-3H-pyrazol-3-one (P6) and (Z)-4-(2-(4-bromophenyl)hydrazineylidene)-5-phenyl,4-trifluoromethylphenyl-2,4-dihydro-3H-pyrazol-3-one (P5) showed a significant inhibition profile against hCA II with K_i values of 16.1 ± 2.8 and 22.1 ± 3.7 nM, respectively (Table 1 and Figure 3).

Recently, the most prescribed ChEIs are donepezil, galantamine, and rivastigmine. Galantamine and donepezil have brief-rolling reversible competitive inhibitors, whereas rivastigmine is actively reacted by ChE.^[46] However, rivastigmine has an equal affinity for AChE enzyme and that is very momentous drug, which is prescribed for the therapy of AD.^[47] It showed well which phenothiazines were observed to inhibit ChE, especially AChE.^[48] This important enzyme was very strongly inhibited by novel pyrazoline derivatives (P1–7; Table 1 and Figure 4). These new molecules had K_i values ranging from 48.2 ± 9.45 to 84.1 ± 17.2 nM for AChE. Additionally, TAC compound, used as standard inhibitor, had K_i value of 89.5 ± 11.1 nM toward AChE. In this study, all the evaluated novel pyrazoline derivatives (P1–7) showed potent inhibition against AChE enzyme, but the compound of (Z)-4-(2-(4-bromophenyl)hydrazineylidene)-5-phenyl,4-trifluoromethylphenyl-2,4-dihydro-3H-pyrazol-3-one (P5) and (Z)-4-(2-(4-bromophenyl)hydrazineylidene)-5-phenyl-2-(2,4,6-tri-

chlorophenyl)-2,4-dihydro-3H-pyrazol-3-one (P6), which showed excellent inhibition profile against AChE with K_i values of 48.15 ± 9.45 and 52.65 ± 15.38 nM, respectively (Figures 2 and 3).

CA enzymes have seven diverse enzyme families: the α -, β -, γ -, δ -, ζ -, η and θ -CA. α -CA enzymes have usually scarcely dimer form and monomer structures.^[49] β -CAs (in prokaryotes) are tetramers or octamers, dimer forms, γ -CAs (in archaea) are trimers, whereas the ζ and δ -CAs (in marine diatoms) are less well understood up to now.^[50] All human hCAs have belonged to the α -class. So far, 16 isoenzymes have been discovered.^[51] All of CA classes are metalloenzymes, which have Zn^{2+} , Cd^{2+} , or Fe^{2+} at their enzyme active sites.^[52] Various isozymes of CA have been defined as remedial purpose for different diseases. Indeed, the plan of isoenzyme-specific inhibitors is searched for the development of improved treatments. CAIs were classified into two principal groups, the metal complexing anions and the unsubstituted sulfonamides. Sulfonamide molecules are very momentous CAIs and sulfamide compounds are effective organic drugs in medical chemistry.^[53] The therapy of AD centralized on AChE inhibitor (AChEI) compounds, such as TAC, rivastigmine, galantamine, and donepezil.^[54] However, in 2013, it was determined that it caused liver damage. Therefore, the most important side effect is liver damage other than those mentioned above.^[55] AD is defined as a complex syndrome where diverse factors are accountable for its etiology like

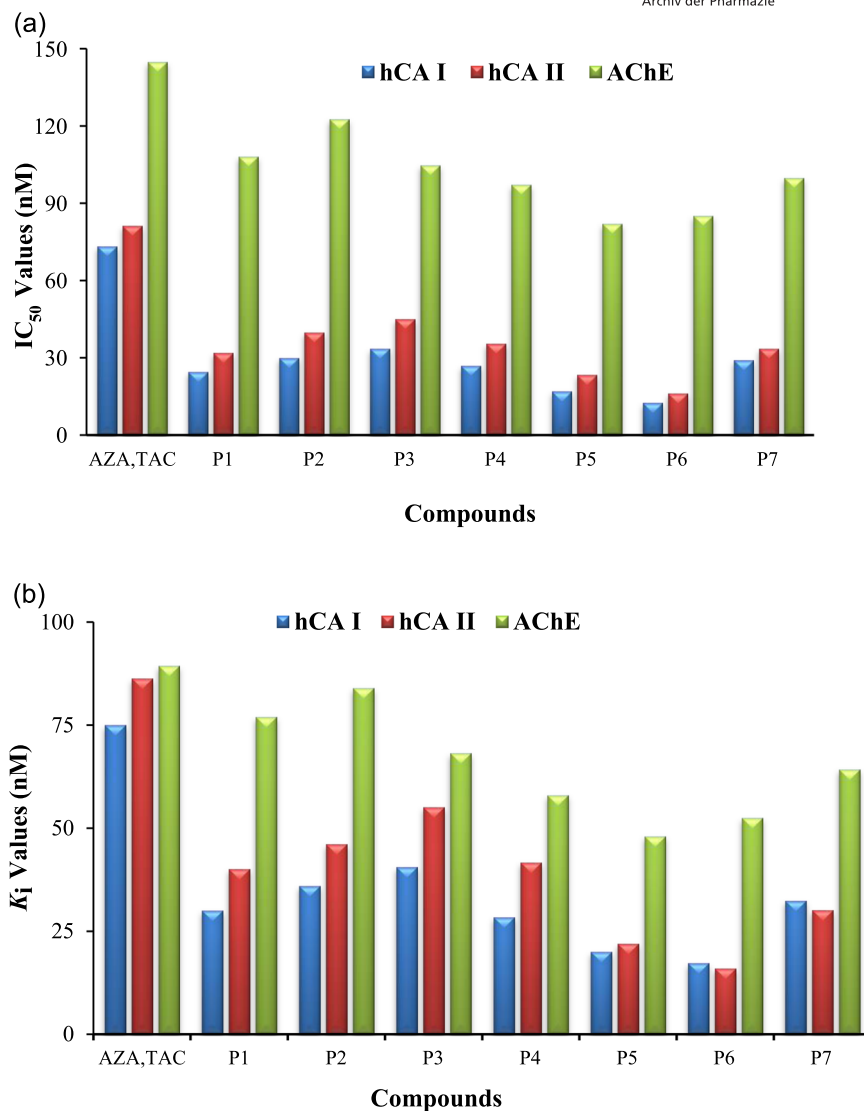


FIGURE 3 (a) IC₅₀ values for novel pyrazoline derivatives (P1–7) against hCA I and II, and AChE enzyme. (b) K_i values for novel pyrazoline derivatives (P1–7) against hCA I and II and AChE enzyme. AChE: acetylcholinesterase; hCA I and II: human carbonic anhydrase isoenzymes I and II

β-amyloid aggregation, low levels of ACh, and tau protein aggregation.^[56] AChEIs are used in the treatment of multiple neuromuscular diseases, in addition, were searched for therapy of AD. AChE accelerates the hydrolysis and involves the regulation of ACh.^[57]

Anticonvulsant drugs such as topiramate AZA and zonisamide were recorded CA inhibitors.^[58] CA enzymes are classical which are inhibited by different compounds with a sulfonamide-based (SO₂NH₂) zinc-binding group or their bioisosteres such as sulfamides and sulfamates. As CA II enzymes are the most physiologically plentiful isoforms, which they were mostly recorded as the predominant off-purpose isozymes of which inhibitions were eschewed.^[59] Recently, multiple kinds of compounds have been searched as nonclassical CAIs, including polyamines, coumarins, phenols, carboxylic acids, fullerenes, and their derivatives.^[60]

2.3 | In silico studies

The physicochemical properties of the synthesized compounds such as molecular weight, number of hydrogen bond acceptor and donor,

partition coefficient, percent human oral absorption, and solvent accessible surface area (SASA) were screened using QikProp module. The properties were analyzed through ADME (absorption, distribution, metabolism, and excretion) risk screening study and Lipinski's rule of five. The data have been presented in Table 2. Compound should meet Lipinski's rule of five including MW < 500 kDa, donor HB < 5, accept HB < 10, and logP_{w/o} < 5 to possess drug-like characteristics^[61] and also it should meet SASA and percent human oral absorption values. As shown in Table 2, all synthesized compounds were consistent with almost all these rules. Lipophilicity (logP_{w/o}) value of all synthesized compounds was in range from 3.54 to 6.86. Molecular weight and percent oral absorption of all synthesized compound are within the range, 343.18–522.62 and 58.32–100, respectively. The compounds were found with optimum number of hydrogen bond donors (0–1) and acceptors (4.5–6.5). SASA value in Å² was from 618.24 to 805.58, which were within the range.

The primary binding site on receptors is often known from the structure of a cocrystallized complex. In some instances, however,

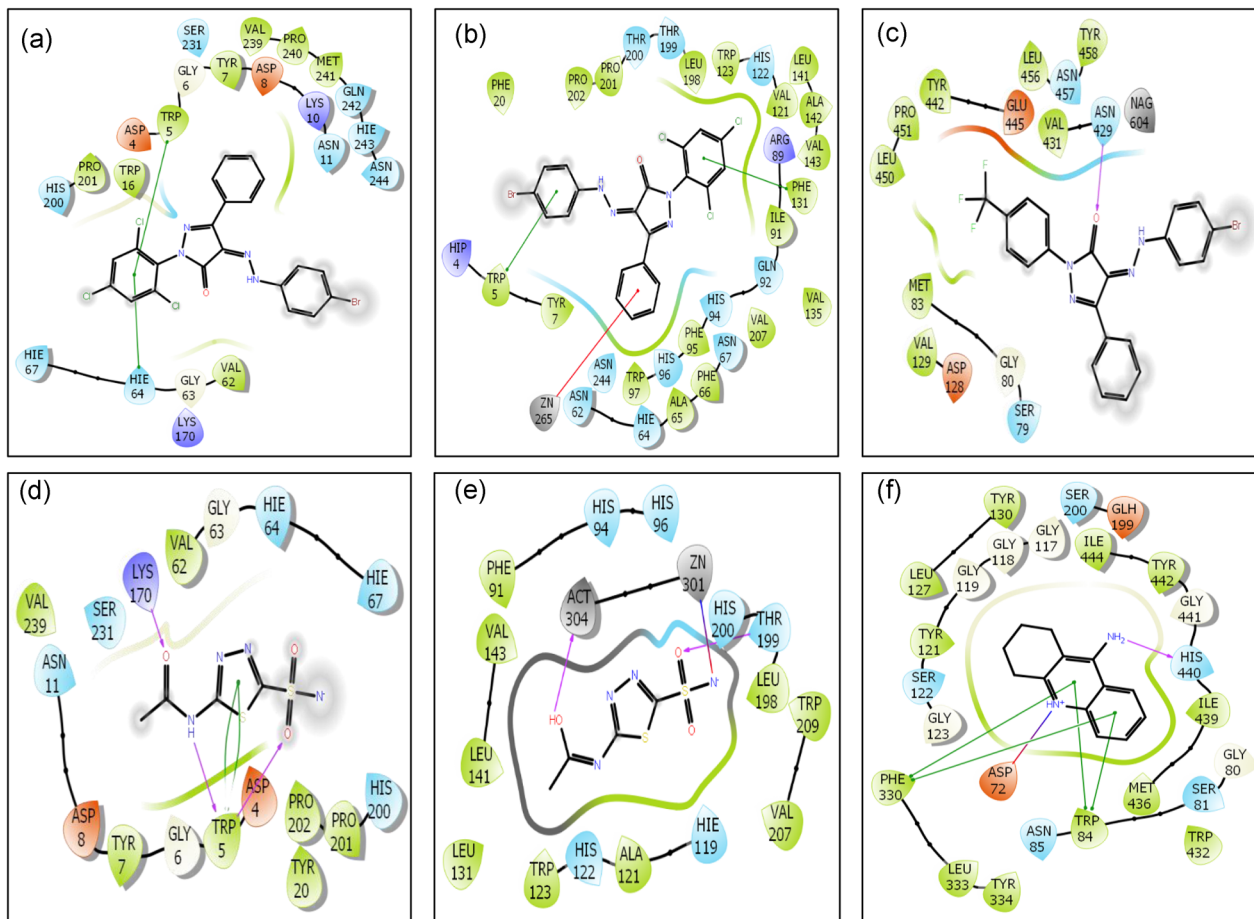


FIGURE 4 Two-dimensional receptor–ligand interaction diagram; (a) P6-hCA I, (b) P6-hCA II, (c) P5-AChE, (d) AZA-hCA I, (e) AZA-hCA II, and (f) TAC-AChE. AChE: acetylcholinesterase; hCA: human carbonic anhydrase

the location of a binding site for protein–ligand or protein–protein interactions is not exactly known even though the protein structures are available. So, we identified likely binding sites of the receptors with SiteScore and Dscore obtained from SiteMap module. We found three binding sites for hCA I and II receptors and four binding sites for AChE receptor. The site with highest SiteScore and Dscore was considered and chosen as druggable site.

To identify the binding mechanism of the synthesized pyrazoline derivatives against hCA I, hCA II, and AChE enzymes. We carried out

molecular docking simulation studies of the synthesized compounds using Glide docking and induced fit docking (IFD) methodologies. All receptors to be used for docking studies were chosen due to their low resolution. Briefly, all ligands were first docked on the binding sites of the receptors using the Glide docking methodologies. Docking and Glide scores of predicted best binding pose of ligands and standard inhibitors were shown in Table 3. P5, P3 and P2 compounds exhibited higher negative Glide score than other pyrazoline derivatives docked onto hCA I, hCA II, and AChE,

TABLE 2 Predicted physicochemical data of the pyrazoline derivatives

Compound	MW	DonorHB	AcptHB	LogP _{w/o}	Percent oral absorption	SASA
P1	343.18	1	4.5	3.54	100	618.24
P2	419.28	0	4.5	5.33	100	684.61
P3	447.33	0	4.5	6.49	100	803.62
P4	447.33	0	4.5	5.87	100	731.89
P5	487.28	0	4.5	6.86	100	805.58
P6	522.62	0	4.5	6.74	100	739.85
P7	509.28	0	6.5	3.97	58.32	743.98

Note: AcptHB: H-bond acceptors; DonorHB: H-bond donor; logP_{w/o}: predicted octanol/water partition coefficient; percent oral absorption: predicted human oral absorption on 0–100% scale; MW: molecular weight; SASA: total solvent accessible surface area.

respectively. According to in vitro inhibition studies, all pyrazoline derivatives exhibited potent inhibitory activities against hCA I, hCA II, and AChE enzyme as in docking studies. After Glide docking experiments, the best active inhibitor-compounds for each receptor were selected for IFD methodology and the compounds were docked onto the binding sites of the receptors. Two-dimensional ligand interaction diagram of best-posed compounds and reference inhibitors were presented in Figure 4. The compounds formed some important interactions with binding site residues of receptors. Two-dimensional interaction diagrams have shown that the selected compounds and the reference inhibitors interacted with and are surrounded by similar residues of receptors.

The lowest energy poses for the selected compounds on the binding site of hCA I, hCA II, and AChE were presented in Figure 5. The P6 compound well located to the binding sites of hCA I and II as seen in Figure 5a,b. But P6 compound was not H-bonded with any residues in the binding site of hCA I. However, it formed π - π stacking with the side-chain atoms of Trp5 and His64 residues. The compound similarly did not form any hydrogen bond interactions with the binding site of hCA II. The compound formed π - π stacking with the side-chain atoms of Trp5 and Phe131 residues. Moreover, the compound formed π interaction between ligands and Zn atom. Of the most active compound, P5 well located to the binding sites of AChE. The compound exhibited one hydrogen bond interaction with Asn429 residue of the receptor as seen Figure 5c.

Not only is active against a target but also possess adequate ADME properties is required for a molecule to be considered as a drug. Hence, ADME properties are important in drug discovery and development studies. All the synthesized compounds passed most of the ADME test. Of the most active compound, P5 and P6 slightly exceeded MW and $\log P_{w/o}$ values. But, all compounds meet optimum parameters for drug-likeness according to Qik-prop predictions.

Therefore, the synthesized pyrazoline derivatives can be considered as drug-like molecules. To illustrate theoretically inhibiting mechanism of potential compounds P1-7, further Glide docking and IFD studies were performed on hCA I, hCA II, and AChE receptors. In Glide docking studies, we detected that all compounds exhibited high affinities on three receptors compared with standard inhibitors for the receptors. Glide docking suggested that all ligands were active inhibitor as in the in vitro experiment results. After these findings, we focused on inhibiting mechanism of most active compounds determined from the in vitro experiments and observed that best-scored poses of the compounds well located in detected binding sites of the receptors. On the basis of molecular docking analyses, we detected that Trp5 residue of hCA I, and Zn atom of hCA II are key amino acid and element for inhibition of these enzymes.

3 | CONCLUSION

We synthesized novel 3H-pyrazol-3-one derivatives and their structures were determined by spectroscopic methods. All of the synthesized compounds effectively inhibited some metabolic enzymes such as AChE, CA I and II, at the nanomolar levels. As we considered above, novel pyrazoline derivatives (P1-7) can be good inhibitors, for CAIs and AChEIs.

4 | EXPERIMENTAL

4.1 | Chemistry

4.1.1 | General

All the used chemical materials were purchased from Merck (Darmstadt, Germany) and Sigma-Aldrich (Steinheim, Germany) companies. The

TABLE 3 Glide and IFD scores (kcal/mol) of the pyrazoline derivatives in the catalytic sites of hCA I, hCA II, and AChE

Compounds	hCA I			hCA II			AChE		
	Glide XP		IFD	Glide XP		IFD	Glide XP		IFD
	Docking score	Glide score		Docking score	Glide score		Docking score	Glide score	
P1	-3.251	-4.157	-	-3.183	-4.088	-	-7.909	-8.815	-
P2	-4.693	-4.762	-	-3.519	-4.821	-	-9.915	-9.985	-
P3	-4.415	-4.474	-	-3.558	-4.950	-	-8.802	-8.862	-
P4	-5.201	-5.258	-	-4.343	-4.400	-	-8.776	-8.803	-
P5	-5.385	-5.442	-	-3.231	-4.644	-	-8.076	-8.133	-4.679
P6	-3.792	-3.934	-5.029	-3.701	-4.617	-7.034	-7.906	-8.048	-
P7	-4.172	-4.432	-	-3.683	-4.297	-	-8.927	-9.186	-
AZA ^a	-4.447	-5.787	-	-6.982	-8.417	-	-	-	-
TAC ^b	-	-	-	-	-	-	-10.581	10.582	-

Note: AChE: acetylcholinesterase; AZA: acetazolamide; hCA: human carbonic anhydrase; TAC: tacrine.

^aAZA was used as a standard inhibitor for hCA I and II.

^bTAC was used as a standard inhibitor for AChE enzyme.

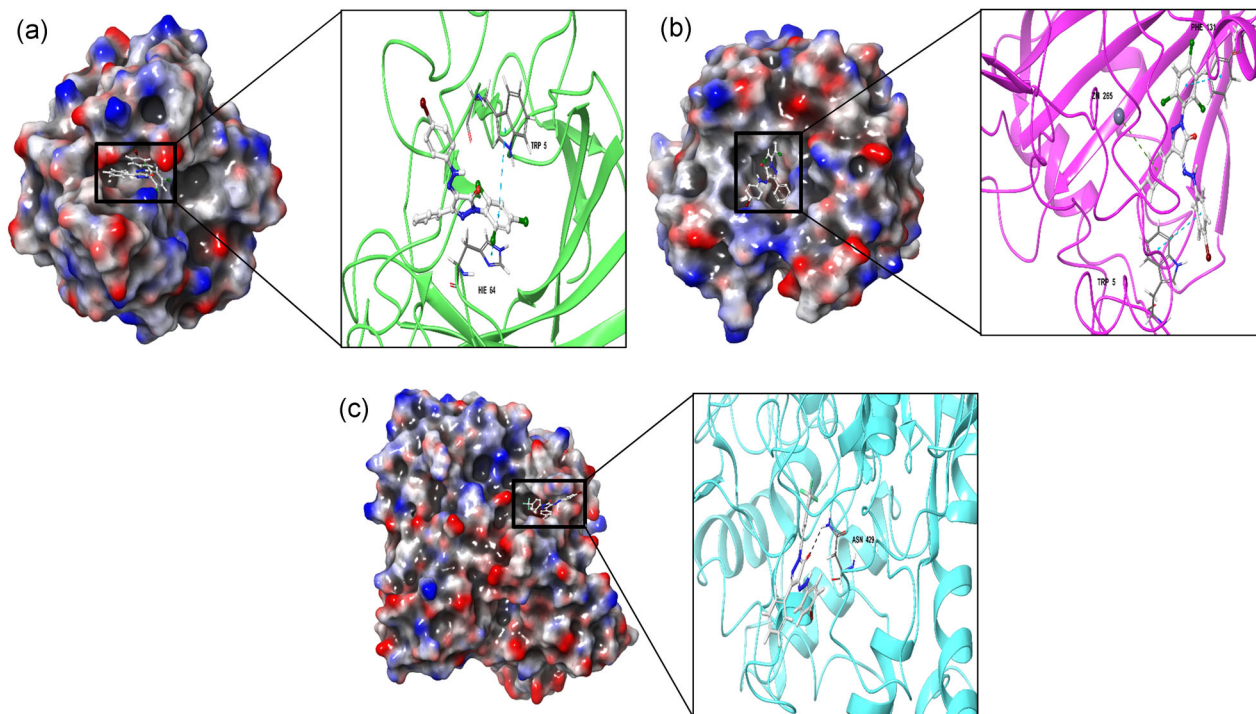


FIGURE 5 Best-scored docking pose of (a) P6, (b) P6, and (c) P5 compounds inside catalytic side of the hCA I, hCA II, and AChE receptors, respectively. Key amino acid and element were determined in the 3D positions in active sites. Ligands are represented as white ball-and-stick, interacted residues are represented as gray ball-and-stick. hCA I, hCA II, and AChE receptors are represented as green, pink and blue cartoon, respectively. AChE: acetylcholinesterase; hCA: human carbonic anhydrase

structures of obtained compounds were determined by ^1H (400 MHz), ^{13}C (100 MHz), and ^{19}F (500 MHz) NMR spectra on a Bruker DRX-400 high performance digital FT-NMR spectrometer from Japan. The infrared spectra were recorded on a PerkinElmer Precisely Spectrum one spectrometer using pressed disc in the range of $4000\text{--}450\text{ cm}^{-1}$ at Mus Alparslan University Scientific and Technological Research Central. The mass spectrum was measured on Thermo Fisher Scientific TSQ-Quantum Access LC/MS spectrometers from Japan. Melting points of these compounds were determined on an Electrothermal Gallenkamp apparatus and are uncorrected at Mus Alparslan University Scientific and Technological Research Central. The obtained compounds were done checking the purity and follow up of the reactions tested in each step by thin layer chromatography (TLC) SiO_2 using a DC Alufolien Kieselgel 60F 254 Merck. These compounds were visualized by Camag TLC devices.

The InChI codes of the investigated compounds together with some biological activity data are provided as Supporting Information.

Ethyl 2-((4-bromophenyl)diazenyl)-3-oxo-phenylpropanoate (1)

4-Bromo aniline (0.172 g, 1 mmol) was dissolved in concentrated sulfuric acid (1 mmol) and NaNO_2 (0.2 g, 3 mmol) was dissolved in 20 ml water. These solutions were kept in ice bath for 10 min below 0°C and then NaNO_2 solution was added dropwise to the solution of 4-bromo aniline over a period of 30 min with constant stirring at 0°C . The diazonium salt of 4-bromo aniline generated was immediately

used for coupling reaction with ethyl benzoylacetate (0.163 g, 1 mmol). The ethyl benzoylacetate was taken in 10 ml methanol. The solution was added dropwise to the solution of diazonium salt over a period 30 min with continuous stirring below 0°C . The reaction was allowed to cool to ambient temperature. The mixture was stirred 12 h. The product was washed with water. It was filtered and dried. Then, it was crystallized from acetone. Yield: 84%. Mp. $136\text{--}138^\circ\text{C}$, FT-IR (ν , cm^{-1}): 3125, 3065, 2945, 1721, 1670, 1604, 1492, 1444, 1332. $^1\text{H-NMR}$ (400 MHz, $\text{DMSO-}d_6$) δ (ppm): 8.3 (s, 1H, -NH), 8.0–6.6 (m, 9H, Ar-H), 3.9 (q, $J = 9.6$ Hz, 2H, $-\text{CH}_2$), 1.2 (t, $J = 5.8$ Hz, 3H, $-\text{CH}_3$). $^{13}\text{C-NMR}$ (100 MHz, $\text{DMSO-}d_6$) δ (ppm): 191.54, 164.4, 150.7, 143.5, 141.1, 136.2, 132.1, 129.5, 128.7, 128.3, 127.1, 120.6, 110.1, 59.7, 13.4.

4.1.2 | General procedure for the synthesis of novel pyrazoline derivatives

The starting material 1 (0.5 mmol) and sulfuric acid (0.05 mmol) were dissolved in ethanol (10 mL). The appropriate hydrazines (0.5 mmol) were added in the prepared solution and then, it was refluxed for 6 h. The reaction process was followed by TLC using ethyl acetate/*n*-hexane (1:5) as solvent eluent system. After completion reaction, the mixture was allowed to cool ambient temperature. The precipitated product was filtered. The products were crystallized from toluene.

(Z)-4-(2-(4-Bromophenyl)hydrazineylidene)-5-phenyl-2,4-dihydro-3H-pyrazol-3-one (P1)

P1 was synthesized according to the general procedure. Yield: 64%. Mp. 198–200°C; FT-IR (ν , cm^{-1}): 3184, 3125, 3065, 1670, 1600, 1492–1444, 1332; (+)ESI-HRMS m/z : calculated for $[\text{C}_{15}\text{H}_{11}\text{BrN}_4\text{O}+\text{H}^+]$: 344.1839; observed 344.1846. $^1\text{H-NMR}$ (400 MHz, $\text{DMSO-}d_6$) δ (ppm): 8.3 (s, 1H, -NH), 8.0–6.6 (m, 9H, Ar-H). $^{13}\text{C-NMR}$ (100 MHz, $\text{DMSO-}d_6$) δ (ppm): 163.6, 159.6, 157.3, 141.3, 135.5, 132.2, 130.5, 129.8, 128.5, 127.5, 122.2.

(Z)-4-(2-(4-Bromophenyl)hydrazineylidene)-2,5-diphenyl-2,4-dihydro-3H-pyrazol-3-one (P2)

P2 was synthesized according to the general procedure. Yield: 70%. Mp. 212–214°C; FT-IR (ν , cm^{-1}): 3226, 3080, 1666, 1610, 1496–1442, 1315; (+)ESI-HRMS m/z : calculated for $[\text{C}_{21}\text{H}_{15}\text{BrN}_4\text{O}+\text{H}^+]$: 420.2775; observed 420.2786; $^1\text{H-NMR}$ (400 MHz, $\text{DMSO-}d_6$) δ (ppm): 8.3 (s, 1H, -NH), 7.9–6.5 (m, 14H, Ar-H); $^{13}\text{C-NMR}$ (100 MHz, $\text{DMSO-}d_6$) δ (ppm): 161.5, 155.2, 152.8, 143.5, 136.5, 131.3, 130.5, 129.6, 129.0, 128.5, 121.6, 119.7.

(Z)-4-(2-(4-Bromophenyl)hydrazineylidene)-5-phenyl,2,5-dimethylphenyl-2,4-dihydro-3H-pyrazol-3-one (P3)

P3 was synthesized according to the general procedure. Yield: 56%. Mp. 216–218°C; FT-IR (ν , cm^{-1}): 3157, 3082, 1672, 1610, 1498–1442, 1321; (+)ESI-HRMS m/z : calculated for $[\text{C}_{23}\text{H}_{19}\text{BrN}_4\text{O}+\text{H}^+]$: 448.3381; observed 448.3386; $^1\text{H-NMR}$ (400 MHz, $\text{DMSO-}d_6$) δ (ppm): 8.1 (s, 1H, -NH), 7.9–6.6 (m, 12H, Ar-H), 2.3 (s, 3H, CH_3), 1.5 (s, 3H, CH_3); $^{13}\text{C-NMR}$ (100 MHz, $\text{DMSO-}d_6$) δ (ppm): 156.3, 152.7, 143.2, 142.3, 139.0, 135.4, 135.1, 131.7, 130.9, 130.5, 129.9, 129.2, 128.2, 127.5, 126.9, 125.1, 124.4, 122.4, 118.4, 21.5, 16.6.

(Z)-4-(2-(4-Bromophenyl)hydrazineylidene)-5-phenyl,3,4-dimethylphenyl-2,4-dihydro-3H-pyrazol-3-one (P4)

P4 was synthesized according to the general procedure. Yield: 58%. Mp. 222–224°C; FT-IR (ν , cm^{-1}): 3145, 3065, 1662, 1610, 1496–1443, 1318; (+)ESI-HRMS m/z : calculated for $[\text{C}_{23}\text{H}_{19}\text{BrN}_4\text{O}+\text{H}^+]$: 448.3386; observed 448.3387; $^1\text{H-NMR}$ (400 MHz, $\text{DMSO-}d_6$) δ (ppm): 8.1 (s, 1H, -NH), 7.9–6.5 (m, 12H, Ar-H) 2.4 (s, 3H, CH_3), 1.6 (s, 3H, CH_3); $^{13}\text{C-NMR}$ (100 MHz, $\text{DMSO-}d_6$) δ (ppm): 155.3, 153.1, 145.9, 143.5, 141.6, 140.7, 135.4, 132.4, 132.0, 130.8, 130.2, 130.0, 129.6, 129.2, 127.8, 126.1, 125.1, 124.0, 123.3, 119.4, 23.4, 16.3.

(Z)-4-(2-(4-Bromophenyl)hydrazineylidene)-5-phenyl,4-trifluoromethylphenyl-2,4-dihydro-3H-pyrazol-3-one (P5)

P5 was synthesized according to the general procedure. Yield: 65%. Mp. 228–230°C; FT-IR (ν , cm^{-1}): 3184, 3064, 1664, 1598, 1497–1444, 1321; (+)ESI-HRMS m/z : calculated for $[\text{C}_{22}\text{H}_{14}\text{BrF}_3\text{N}_4\text{O}+\text{H}^+]$: 488.2283; observed 488.2292; $^1\text{H-NMR}$ (400 MHz, $\text{DMSO-}d_6$) δ (ppm): 8.1 (s, 1H, -NH), 7.8–6.5 (m, 13H, Ar-H); $^{13}\text{C-NMR}$ (100 MHz, $\text{DMSO-}d_6$) δ (ppm): 156.6, 153.7, 146.9, 142.9, 137.2, 136.5, 135.4, 132.0, 131.4, 130.7, 130.2, 129.6, 129.2, 128.5, 126.8, 125.8, 124.7, 124.4, 123.7, 122.7, 122.1, 118.1. $^{19}\text{F-NMR}$ (470 MHz, $\text{DMSO-}d_6$) δ (ppm) δ -62.55.

(Z)-4-(2-(4-Bromophenyl)hydrazineylidene)-5-phenyl-2-(2,4,6-trichlorophenyl)-2,4-dihydro-3H-pyrazol-3-one (P6)

P6 was synthesized according to the general procedure. Yield: 40%. Mp. 232–234°C; FT-IR (ν , cm^{-1}): 3124, 3065, 1662, 1604, 1498–1443, 1317; (+)ESI-HRMS m/z : calculated for $[\text{C}_{21}\text{H}_{12}\text{BrCl}_3\text{N}_4\text{O}+\text{H}^+]$: 523.6215; observed 523.6224; $^1\text{H-NMR}$ (400 MHz, $\text{DMSO-}d_6$) δ (ppm): 8.0 (s, 1H, -NH), 7.9–6.5 (m, 11H, Ar-H); $^{13}\text{C-NMR}$ (100 MHz, $\text{DMSO-}d_6$) δ (ppm): 160.2, 156.6, 153.4, 146.3, 145.6, 141.6, 141.2, 137.9, 137.9, 134.7, 132.0, 130.8, 130.2, 129.6, 129.2, 128.9, 127.8, 121.7, 120.4, 119.5.

(Z)-4-(2-(4-Bromophenyl)hydrazineylidene)-5-phenyl,2,4-dinitrophenyl-2,4-dihydro-3H-pyrazol-3-one (P7)

P7 was synthesized according to the general procedure. Yield: 62%. Mp. 219–221°C; FT-IR (ν , cm^{-1}): 3155, 3066, 1664, 1608, 1497–1443, 1321; (+)ESI-HRMS m/z : calculated for $[\text{C}_{21}\text{H}_{13}\text{BrN}_6\text{O}_5+\text{H}^+]$: 510.2803; observed 510.2804; $^1\text{H-NMR}$ (400 MHz, $\text{DMSO-}d_6$) δ (ppm): 8.1 (s, 1H, -NH), 8.0–6.5 (m, 12H, Ar-H); $^{13}\text{C-NMR}$ (100 MHz, $\text{DMSO-}d_6$) δ (ppm): 162.5, 156.3, 152.6, 144.1, 141.3, 136.3, 131.8, 130.6, 130.3, 129.8, 129.0, 128.5, 127.5, 126.5, 125.8, 124.7, 124.5, 124.1, 123.1, 122.4, 118.8.

4.2 | Biochemical studies

4.2.1 | hCA isoenzyme purification and inhibition studies

Both hCA isoenzymes from human erythrocytes were purified via a simple single-step by method sepharose-4B-L-tyrosine-sulfanilamide affinity gel chromatography.^[62] For this purpose, the human erythrocyte samples were centrifuged at 13,000 rpm for 25 min. Then, the solution was filtered to remove precipitate. Both hCA isoenzymes were isolated from the serum, which its pH was adjusted to 8.7 by adding solid Tris.^[63] The affinity column was equilibrated by buffer solution (25 mM Tris-HCl/0.1 M Na_2SO_4) at the pH 8.7. The serum was loaded to affinity gel and washed with buffer solution (25 mM Tris-HCl/22 mM Na_2SO_4) at the pH 8.7. The hCA I isoenzyme was eluted by buffer solution (1.0 M NaCl/0.25 M sodium phosphate at the pH 6.3).^[64] On the other hand, hCA II isoenzyme was eluted by another buffer solution (0.1 M CH_3COONa /0.5 M NaClO_4) at the pH 5.6). Both isoenzymes were taken from the column in fractions of 2 ml. All works were realized at 4°C.^[65] The hCA isoenzymes activity were measured by following the change at absorbance specific (348 nm) of *p*-nitrophenyl acetate (PNA) to *p*-nitrophenolate ion over a period of 3 min at room temperature (25°C) using a spectrophotometer (UV-Vis spectrophotometer; Thermo Fisher Scientific) according to the method of Verpoorte et al.^[66] There was 0.4 ml of 0.05 M Tris- SO_4 buffer (pH 7.4), 0.3 ml of 3 mM PNA, 0.2 ml of H_2O , and 0.1 ml of enzyme solution in a test tube content of this reaction.^[67]

4.2.2 | AChE inhibition study

The inhibitory effects of novel pyrazoline derivatives (**P1–7**) on AChE activity were performed according to the spectrophotometric

method of Ellman et al.^[68] Acetylthiocholine iodide (AChI) substrate was utilized for the inhibition act and enzymatic reaction. 5,5'-Dithio-bis(2-nitro-benzoic) acid (DTNB) compound was utilized in this study for the measurement of the AChE activity.^[69] Briefly, 750 μ l of sample solution dissolved in deionized water at different concentrations with 100 μ l of Tris/HCl buffer (1.0 M, pH 8.0), and 50 μ l of AChE solution were mixed and incubated for 64 min at 21°C.^[70] The reaction was initiated by the addition of 50 μ l of AChI. Then, 50 μ l of DTNB (0.5 mM) was added. The hydrolysis of these substrates was monitored spectrophotometrically by formation of the yellow 5-thio-2-nitrobenzoate anion as the result of the reaction of thiocholine with DTNB, released by enzymatic hydrolysis of AChI, with an absorption maximum at a wavelength of 412 nm.^[71] For the computation of K_i values of these compounds, three diverse novel pyrazoline derivatives (P1-7) concentrations were utilized. One AChE enzyme unit is the amount of enzyme that hydrolyzes 1.0 mol of AChI to choline and acetate per minute at pH 8.0 at 37°C,^[72] and Lineweaver-Burk curves were drawn.^[73]

4.3 | In silico studies

4.3.1 | Ligand preparation

Molecular docking studies were performed with Small Drug Discovery Suites package (Schrödinger 2017-2, LLC). Two-dimensional structures of the synthesized compounds were sketched and then converted to 3D structures using LigPrep module in Maestro 11.4. To prepare ligands for docking process, the ligands were set to the physiological pH and using OPLS-2005 force field performed energy minimization. The Epik option was used for keeping ligand in the correct protonation state.^[74]

4.3.2 | Prediction of ADME properties

To determine pharmacokinetic properties of all synthesized compounds, ADME test was performed with QikProp module in Maestro 11.4. The test provides information about ADME of the synthesized compounds in comparison to a particular molecule's properties with those of 95% of known drugs. Prepared ligands were used in the calculation of QikProp. The drug-likeness of the compounds were determined with Lipinski's rule of five (mol_MW, log $P_{o/w}$, donorHB, and accptHB).^[74]

4.3.3 | Protein processing and binding site identification

The 3D crystal structures of hCA I, hCA II, and AChE enzymes were obtained from RCSB Protein Data Bank (PDB ID: 2FW4, 5AML, and 4TVK, respectively). The 3D crystal structure was repaired and prepared via protein preparation wizard in Maestro 11.4. First of all, all water molecules were removed from the crystal structure. Bond orders and charges were assigned and then all missing hydrogen atoms were added to protein structure. Amino acids were ionized by setting physiological pH with the help of Propka software. Finally, restrained minimization step has also been performed using OPLC force field. This

minimized structure was the best structure to utilize for molecular docking. After protein preparation, top-ranked potential protein binding sites were identified to determine most suitable binding site of proteins using SiteMap module in Maestro 11.4.^[74]

4.3.4 | Molecular docking studies

Ligand docking was performed for the prediction of best poses and binding energies of ligands at binding sites identified by SiteMap on the receptor. First of all, all ligands were docked on the receptors using Glide docking module in Maestro 11.4. Briefly, grid box was generated around the selected residues at the binding site using the receptor grid generation platform. Then rigid receptor-docking simulations were performed using the standard precision and extra precision options in Maestro 11.4. Following Glide docking, we performed IFD using IFD module in Maestro 11.4. In the IFD experiment, three ligands, which exhibited the most effective inhibition in vitro experiment, were docked on the receptors. Briefly, centroid of the residues was generated around the selected residues at the binding site. After that, side chains were automatically trimmed based on B-factor; closest residues to the ligand were refined within 3.4 Å of ligand pose in prime refinement. Then flexible receptor-docking simulations were performed in Maestro 11.4.^[74]

ACKNOWLEDGEMENTS

This study was supported by Scientific Research Fund of Iğdır University. Project Number: 2018-SBE-A01. A certain part of this study was carried out in Iğdır University Research Laboratory Practice and Research Center.

CONFLICT OF INTERESTS

The authors declare that there are no conflict of interests.

ORCID

Fikret Turkan  <http://orcid.org/0000-0002-0538-3157>

Parham Taslimi  <http://orcid.org/0000-0002-3171-0633>

REFERENCES

- [1] A. Lévai, A. M. S. Silva, J. A. S. Cavaleiro, I. Alkorta, J. Elguero, J. Jekő, *Eur. J. Org. Chem.* **2006**, *12*, 2825.
- [2] A. Saikia, M. G. Barthakur, M. Borthakur, C. J. Saikia, U. Bora, R. C. Boruah, *Tetrahedron Lett.* **2006**, *47*, 43.
- [3] S. D. Joshi, S. R. Dixit, M. N. Kirankumar, T. M. Aminabhavi, K. V. S. N. Raju, R. Narayan, K. S. Yang, *Eur. J. Org. Chem.* **2016**, *107*, 133.
- [4] P. Jeschke, *Pest Manage. Sci.* **2016**, *72*, 433.
- [5] B. Varghese, S. N. Al-Busafi, F. O. Suliman, S. M. Z. Al-Kindy, *RSC Adv.* **2017**, *7*, 46999.
- [6] A. Çetin, i. Bildirici, *J. Saudi Chem. Soc.* **2018**, *22*(3), 279.
- [7] F. Turkan, A. Cetin, P. Taslimi, M. Karaman, i. Gulçin, *Bioorg. Chem.* **2019**, *86*, 420.

- [8] M. S. Shah, S. U. Khan, S. A. Ejaz, S. Afridi, S. U. F. Rizvi, M. Najam-ul-Haq, J. Iqbal, *Biochem. Biophys. Res. Commun.* **2017**, *482*, 615.
- [9] D. Havrylyuk, B. Zimenkovsky, O. Vasylenko, L. Zaprutko, A. Gzella, R. Lesyk, *Eur. J. Org. Chem.* **2009**, *44*, 1396.
- [10] E. Nassar, *J. Am. Sci.* **2010**, *6*, 463.
- [11] M. A. Berghot, E. B. Moawad, *Eur. J. Pharm. Sci.* **2010**, *20*(2), 173.
- [12] N. D. Amnerkar, K. P. Bhusari, *Eur. J. Med. Chem.* **2010**, *45*(1), 149.
- [13] A. Sarkar, S. Rakshit, S. C. Bhattacharya, *J. Photochem. Photobiol.* **2017**, *A 343*, 77.
- [14] N. Kahrman, Z. Haşımoğlu, V. Serdaroğlu, F. Ş. Beriş, B. Barut, N. Yaylı, *Arch. Pharm.* **2017**, *350*, 1600285.
- [15] R. Sadashiva, D. Naral, J. Kudva, N. Shivalingegowda, N. K. Lokanath, K. J. Pampa, *Med. Chem.* **2017**, *26*, 1213.
- [16] H. Bao, Q. Zhang, Z. Zhu, H. Xu, F. Ding, M. Wang, Z. Yan, *Sci. Rep.* **2017**, *7*(1), 9153.
- [17] N. S. Shringare, V. H. Chavan, S. P. Bhale, B. S. Dongare, B. Y. Mule, D. N. Kolekar, P. B. Bandgar, *Croat. Chem. Acta* **2018**, *91*(3), 357.
- [18] I. Khan, M. A. Tantray, M. S. Alam, H. Hamid, *Eur. J. Med. Chem.* **2017**, *125*, 464.
- [19] M. Arnost, A. Pierce, E. ter Haar, D. Lauffer, J. Madden, K. Tanner, J. Green, *Bioorg. Med. Chem. Lett.* **2010**, *20*(5), 1661.
- [20] X. H. Liu, P. Cui, B. A. Song, P. S. Bhadury, H. L. Zhu, S. F. Wang, *Bioorg. Med. Chem.* **2008**, *16*, 4075.
- [21] B. B. Lorenzetti, S. H. Ferreira, *Eur. J. Pharmacol.* **1985**, *114*, 375.
- [22] G. Dowling, E. Malone, *J. Pharm. Biomed. Anal.* **2011**, *56*, 359.
- [23] I. Başar, K. Bircan, C. Taşar, A. Ergen, F. Cakmak, D. Remzi, *Int. Urol. Nephrol.* **1991**, *23*(3), 227.
- [24] F. D. Hart, P. L. Boardman, *Br. Med. J.* **1964**, *1*(5397), 1553.
- [25] R. L. Jayaraj, K. Tamilselvam, T. Manivasagam, N. Elangovan, *J. Mol. Neurosci.* **2013**, *51*, 863.
- [26] F. Chimenti, B. Bizzarri, F. Manna, A. Bolasco, D. Secci, P. Chimenti, M. I. Brenciaglia, *Bioorg. Med. Chem. Lett.* **2005**, *15*(3), 603.
- [27] P. Taslimi, İ. Gulcin, B. Ozgeris, S. Goksu, F. Tumer, S. H. Alwasel, C. T. Supuran, *J. Enzyme Inhib. Med. Chem.* **2016**, *31*(1), 152.
- [28] H. İ. Gül, K. Kucukoglu, C. Yamali, S. Bilginer, H. Yuca, İ. Ozturk, P. Taslimi, İ. Gülçin, C. T. Supuran, *J. Enzyme Inhib. Med. Chem.* **2016**, *31*(4), 568.
- [29] A. Behcet, T. Çağlılar, D. Barut Celepci, A. Aktaş, P. Taslimi, Y. Gök, M. Aygün, R. Kaya, İ. Gülçin, *J. Mol. Struct.* **2018**, *1170*, 160.
- [30] P. Taslimi, İ. Gülçin, N. Öztaşkın, Y. Çetinkaya, S. Göksu, S. H. Alwasel, C. T. Supuran, *J. Enzyme Inhib. Med. Chem.* **2016**, *31*(4), 603.
- [31] B. Ozgeriş, S. Göksu, L. Köse Polat, İ. Gülçin, R. E. Salmas, S. Durdagi, F. Tümer, C. T. Supuran, *Bioorg. Med. Chem.* **2016**, *24*(10), 2318.
- [32] M. Boztaş, Y. Çetinkaya, M. Topal, İ. Gülçin, A. Menzek, E. Şahin, M. Tanc, C. T. Supuran, *J. Med. Chem.* **2015**, *58*(2), 640.
- [33] A. Yıldırım, U. Atmaca, A. Keskin, M. Topal, M. Çelik, İ. Gülçin, C. T. Supuran, *Bioorg. Med. Chem.* **2015**, *23*(10), 2598.
- [34] M. Rezaei, Ç. Bayrak, P. Taslimi, İ. Gülçin, A. Menzek, *Turk. J. Chem.* **2018**, *42*(3), 808.
- [35] Z. Huyut, S. Beydemir, İ. Gülçin, *J. Enzyme Inhib. Med. Chem.* **2016**, *31*(6), 1234.
- [36] L. Polat Köse, İ. Gülçin, A. C. Gören, J. Namiesnik, A. L. Martinez-Ayala, S. Gorinstein, *Ind. Crops Prod.* **2015**, *74*, 712.
- [37] D. Ozmen Ozgun, C. Yamali, H. İ. Gül, P. Taslimi, İ. Gülçin, T. Yanik, C. T. Supuran, *J. Enzyme Inhib. Med. Chem.* **2016**, *31*(6), 1498.
- [38] A. Sujayev, E. Garibov, P. Taslimi, İ. Gülçin, S. Gojayeve, V. Farzaliyev, S. H. Alwasel, C. T. Supuran, *J. Enzyme Inhib. Med. Chem.* **2016**, *31*(6), 1531.
- [39] B. Turan, K. Sendil, E. Sengul, M. S. Gultekin, P. Taslimi, İ. Gulcin, C. T. Supuran, *J. Enzyme Inhib. Med. Chem.* **2016**, *31*(S1), 79.
- [40] F. Ozbey, P. Taslimi, I. Gulcin, A. Maraş, S. Goksu, C. T. Supuran, *J. Enzyme Inhib. Med. Chem.* **2016**, *31*, 79.
- [41] M. Işık, S. Beydemir, A. Yılmaz, M. E. Naldan, H. E. Aslan, İ. Gülçin, *Biomed. Pharmacother.* **2017**, *87*, 561.
- [42] H. Kurt, A. Çetin, S. Bozari, *J. Inst. Sci. Technol.* **2018**, *8*(2), 223.
- [43] W. Zhao, Z. H. Shen, J. H. Xing, G. Yang, T. M. Xu, W. L. Peng, X. H. Liu, *Chem. Pap.* **2017**, *71*(5), 921.
- [44] P. Taslimi, İ. Gulçin, *J. Food Biochem.* **2018**, *42*(3), e12516.
- [45] M. U. Koçyiğit, P. Taslimi, F. Gurses, S. Soyulu, S. Durna Dastan, İ. Gulçin, *J. Biochem. Mol. Toxicol.* **2018**, *32*, e22031.
- [46] Y. Sari, A. Aktaş, P. Taslimi, Y. Gök, İ. Gulçin, *J. Biochem. Mol. Toxicol.* **2018**, *32*(1), e22009.
- [47] N. Bulut, U. M. Koçyiğit, I. H. Gecibesler, T. Dastan, H. Karci, P. Taslimi, S. Durna Dastan, İ. Gulçin, A. Cetin, *J. Biochem. Mol. Toxicol.* **2018**, *32*(1), e22006.
- [48] G. Gondolova, P. Taslimi, A. Medjidov, V. Farzaliyev, A. Sujayev, H. Mansura, O. Sahin, B. Yalçın, F. Turkan, I. Gulçin, *J. Biochem. Mol. Toxicol.* **2018**, *32*(9), e22197.
- [49] A. Cetin, F. Turkan, P. Taslimi, İ. Gulçin, *J. Biochem. Mol. Toxicol.* **2018**, *33*, e22261.
- [50] P. Taslimi, E. Sujayev, F. Turkan, E. Garibov, Z. Huyut, F. Farzaliyev, S. Mamedova, İ. Gulçin, *J. Biochem. Mol. Toxicol.* **2018**, *32*(2), e22019.
- [51] İ. Gülçin, A. Scozzafava, C. T. Supuran, H. Akıncioğlu, Z. Koksall, F. Turkan, S. Alwasel, *J. Enzyme Inhib. Med. Chem.* **2016**, *31*(6), 1095.
- [52] İ. Gülçin, A. Scozzafava, C. T. Supuran, Z. Koksall, F. Turkan, S. Çetinkaya, Z. Bingöl, Z. Huyut, S. H. Alwasel, *J. Enzyme Inhib. Med. Chem.* **2016**, *31*(6), 1698.
- [53] F. Turkan, Z. Huyut, P. Taslimi, İ. Gulçin, *J. Biochem. Mol. Toxicol.* **2018**, *32*(3), e22041.
- [54] P. Taslimi, C. Çağlayan, F. Farzaliyev, O. Nabyev, A. Sujayev, F. Turkan, R. Kaya, İ. Gulçin, *J. Biochem. Mol. Toxicol.* **2018**, *32*(4), e22042.
- [55] P. Taslimi, S. Osmanova, C. Çağlayan, F. Turkan, S. Sardarova, V. Farzaliyev, A. Sujayev, N. Sadeghian, İ. Gulçin, *J. Biochem. Mol. Toxicol.* **2018**, *32*(9), e22191.
- [56] İ. Gülçin, P. Taslimi, A. Aygün, N. Sadeghiana, E. Bastem, O. I. Küfrevioğlu, F. Türkan, F. Sen, *Int. J. Biol. Macromol.* **2018**, *119*, 741.
- [57] T. Daştan, U. M. Koçyiğit, S. D. Daştan, C. Kiliçkaya, P. Taslimi, Ç. Özge, M. Koparir, A. Çetin, C. Orek, İ. Gulçin, *J. Biochem. Mol. Toxicol.* **2017**, *31*(11), e21971.
- [58] C. Yamali, H. İ. Gül, A. Ece, P. Taslimi, İ. Gulçin, *Chem. Biol. Drug Des.* **2018**, *91*, 854.
- [59] F. Turkan, A. Cetin, P. Taslimi, I. Gulçin, *Arch. Pharm.* **2018**, *351*(10), 1800200.
- [60] S. Burmaoglu, A. O. Yilmaz, P. Taslimi, O. Algul, D. Kılıç, İ. Gulçin, *Arch. Pharm.* **2018**, *351*, e1700314.
- [61] C. A. Lipinski, F. Lombardo, B. W. Dominy, P. J. Feeney, *Adv. Drug Deliv. Rev.* **2001**, *46*(1-3), 3.
- [62] E. Garibov, P. Taslimi, A. Sujayev, Z. Bingöl, S. Çetinkaya, İ. Gulcin, S. Beydemir, V. Farzaliyev, S. H. Alwasel, C. T. Supuran, *J. Enzyme Inhib. Med. Chem.* **2016**, *31*, 1.
- [63] K. Aksu, B. Özgeris, P. Taslimi, A. Naderi, İ. Gülçin, S. Göksu, *Arch. Pharm.* **2016**, *349*, 944.
- [64] P. Taslimi, A. Sujayev, S. Mamedova, P. Kalin, I. Gulcin, N. Sadeghian, S. Beydemir, İ. Ö. Küfrevioğlu, S. H. Alwasel, V. Farzaliyev, S. Mamedov, *J. Enzyme Inhib. Med. Chem.* **2017**, *32*(1), 137.
- [65] H. I. Gul, E. Mete, P. Taslimi, I. Gulcin, C. T. Supuran, *J. Enzyme Inhib. Med. Chem.* **2017**, *32*, 189.
- [66] J. A. Verpoorte, S. Mehta, J. T. Edsall, *J. Bio. Chem.* **1967**, *242*, 4221.
- [67] H. I. Gul, A. Demirtas, G. Ucar, P. Taslimi, İ. Gülçin, *Lett. Drug Des. Discov.* **2017**, *14*, 573.
- [68] G. L. Ellman, K. D. Courtney, V. Andres, R. M. Featherston, *Biochem. Pharmacol.* **1961**, *7*, 88.
- [69] Ç. Bayrak, P. Taslimi, İ. Gülçin, A. Menzek, *Bioorg. Chem.* **2017**, *72*, 359.
- [70] A. Aktas, P. Taslimi, I. Gulçin, Y. Gök, *Arch. Pharm.* **2017**, *350*, e1700045.
- [71] P. Taslimi, A. Sujayev, E. Garibov, N. Nazarov, Z. Huyut, S. H. Alwasel, İ. Gülçin, *J. Biochem. Mol. Toxicol.* **2017**, *31*, e21897.
- [72] N. Öztaskın, P. Taslimi, A. Maras, S. Göksu, İ. Gülçin, *Bioorg. Chem.* **2017**, *74*, 104.
- [73] H. Lineweaver, D. Burk, *J. Am. Chem. Soc.* **1934**, *56*, 658.

[74] Schrödinger L. Small-Molecule Drug Discovery Suite 2017, December 2018; https://www.schrodinger.com/sites/default/files/s3/mkt/Documentation/2016-4/docs/Documentation.htm#Maestro11_Handbook.html

SUPPORTING INFORMATION

Additional supporting information may be found online in the Supporting Information section at the end of the article.

How to cite this article: Turkan F, Cetin A, Taslimi P, Karaman HS, Gulçin i. Synthesis, characterization, molecular docking and biological activities of novel pyrazoline derivatives. *Arch Pharm Chem Life Sci.* 2019;e1800359
<https://doi.org/10.1002/ardp.201800359>